PROCEEDINGS OF SPIE

SPIEDigitalLibrary.org/conference-proceedings-of-spie

Superdense coding for quantum networking environments

Brian P. Williams, Ronald J. Sadlier, Travis S. Humble

Brian P. Williams, Ronald J. Sadlier, Travis S. Humble, "Superdense coding for quantum networking environments," Proc. SPIE 10547, Advances in Photonics of Quantum Computing, Memory, and Communication XI, 105470B (22 February 2018); doi: 10.1117/12.2295016

SPIE.

Event: SPIE OPTO, 2018, San Francisco, California, United States

Invited Paper

Superdense coding for quantum networking environments

Brian P. Williams[1], Ronald J. Sadlier[1,2], and Travis S. Humble[1]

[1]Oak Ridge National Laboratory, One Bethel Valley Road, Oak Ridge, TN 37831
[2]Bredesen Center, University of Tennessee, Knoxville, Tennessee, 37996

ABSTRACT

Quantum networks provide a versatile infrastructure for communication, computing, and sensing with quantum information. Novel sources and detectors for transmitting and receiving quantum states are critical elements in the development and eventual deployment of robust quantum networks. Alongside performance, the compatibility of quantum network devices with modern networking infrastructure is an important requirement for deployment. We present results on the integration of quantum communication using superdense coding transmitted over optical fiber links into network environments. Our approach takes advantage of a novel complete Bell-state measurement setup that relies on hyper-entanglement in the temporal and polarization degrees of freedom for a two-photon state emitted from a quantum light source. Using linear optics and common single-photon detectors, we record a single-qubit channel capacity of 1.665 ± 0.018. We then demonstrate a full experimental implementation of hybrid, quantum-classical communication protocol for image transfer applications. Our devices integrate with existing fiber optical network and software-defined transmitters and receivers as part of a modular design to provide an extensible quantum communication system that can adapt to future quantum technology goals.

Keywords: Quantum Networks, Quantum Communication

1. INTRODUCTION

Networking is an important aspect of modern communication, computing, and sensor systems that enables modular development and scalable growth. These principles holds true in emerging technologies such as those based on quantum information theory,[1] where networking provides an operationally similar but functionally distinct method of modularity. Quantum networks represent distributed quantum information processing systems composed from computational nodes interconnected by communication links.[2] Quantum networks generalize the principles of quantum information processing systems to include nodes that are not collocated but instead communicate with each other using classical and/or quantum communication. Examples of applications of quantum networks include secure multi-party communication, large-scale quantum computing, and distributed quantum sensing. The design and development of robust and extensible quantum networks is therefore an important goal for future quantum information technology. Notwithstanding efforts to develop robust computational nodes, how these nodes communicate with each other is a central feature for their operation.[3] Recent demonstrations have focused on point-to-point communication or highly specialized purposes, such as QKD networks, and there is an outstanding need to develop networks that can provide more versatile functionality. This includes the ability to reprogram the network purpose as well as to support advanced networking features provided by the use of relays, repeaters, switches, and routers.[4]

Contact information: Brian P. Williams (williamsbp@ornl.gov), Travis S. Humble (humblets@ornl.gov)
This work was supported by the United States Army Research Laboratory.

Advances in Photonics of Quantum Computing, Memory, and Communication XI, edited by Zameer Ul Hasan, Philip R. Hemmer, Alan E. Craig, Alan L. Migdall, Proc. of SPIE Vol. 10547
105470B · © 2018 SPIE · CCC code: 0277-786X/18/$18 · doi: 10.1117/12.2295016

There has been considerable theoretical and experimental effort surrounding the engineering of quantum key distribution (QKD) networks.[5–13] These have been heroic efforts to demonstrate possible quantum communication capabilities even though results from those systems, however, are often specific to QKD applications. While such systems represent fixed-point solutions and, in the broad sense of quantum network science, have limited functionality, they nonetheless emphasize the integration techniques need in quantum networks. However, there is an outstanding need for the development of robust network protocols and abstractions. This is due in part to build networks that provide multiple services and to tailor those services for optimal performance. As a near term example, the on-going development of quantum repeater technologies highlights the need to modify even the most basic protocols for resource efficient quantum communication. These changes are also driven by the discovery of new protocols or use cases that cannot be foreseen during network construction. A longer term goal of establishing ad hoc quantum networks, which enable devices built from different technology bases to interface, will also require control and management methods that are not application or technology specific. The current variability in network components, operation, and behavior motivates our interest in building quantum networks that are programmable and can be modified quickly to take on new tasking.

In this contribution, we present an example of software-defined quantum networking built on the quantum communication protocol of superdense coding.[14,15] Superdense coding enables one qubit to carry two bits of information between a sender Alice and receiver Bob when they share an entanglement resource, perhaps distributed at "off-peak" times.[16] Alice can choose to use this quantum ability at a time of optimal advantage, after the time of distribution, when she and Bob have access to quantum memory.[17] A significant challenge in realizing superdense coding is the need to perform a complete Bell-state measurement (BSM) on the photon pair, which is not possible using only linear optics and a single degree of shared entanglement.[18,19] While nonlinear optics[20] or utilization of ancillary photons and linear optics[21] enable a complete BSM, these methods are challenged by inefficiency and impracticality. However, a complete BSM with linear optics can be performed by using entanglement in an ancillary degree of freedom (DOF), so-called hyperentanglement.[22,23] This ancillary DOF has no information encoded within it, rather, it enables a complete BSM by expanding the measurement space. Complete BSM implementations have been demonstrated previously using states hyperentangled in orbital angular momentum and polarization degrees of freedom[24] as well as with states hyperentangled in momentum and polarization.[25] However, these states are not compatible with transmission through fiber-based networks, which form the backbone of modern telecommunication systems. Previously, Schuck et al. have shown that time-polarization hyperentanglement can be used for a complete BSM,[26] but required number resolving detectors to identify the states completely. Yet this encoding is attractive in that it permits efficient transmission through optical fiber and that some photon pair sources generate time entanglement for "free".

A key feature in the development of our quantum transmitter and receiver is the ability to interface with these network devices using software-defined programming methods. This enables reconfiguration and calibration of the optical system to match end user needs. We provide a demonstration of these ideas using an image transfer application, which involves repeated channel use as well as timing synchronization between the transmitter and receiver. The accuracy with which we recover the transmitted image agrees with the intrinsic error rates of the complete BSM implementation.

2. SUPERDENSE CODING IN AN OPTICAL FIBER NETWORK

Previously, we demonstrated superdense coding over optical fiber links using a complete BSM based on time-polarization hyperentanglement.[15] We review this experiment and discuss improvements that might be made to achieve practical superdense coding within modern fiber-based telecommunication infrastructure.[27] Our experimental configuration for the complete BSM is shown in Fig. 1a. The principle of operation behind the BSM device is to use the temporal and polarization coherences of the photon pair to produce unique detection outcomes for each of the four polarization-encoded Bell states,

$$\left|\Phi^{\pm}\right\rangle = (|H_0H_1\rangle \pm |V_0V_1\rangle)/\sqrt{2} \tag{1}$$

$$\left|\Psi^{\pm}\right\rangle = (|H_0V_1\rangle \pm |V_0H_1\rangle)/\sqrt{2} \tag{2}$$

with H and V denoting horizontal and vertical polarization, respectively, and the subscripts 0 and 1 denote the orthogonal spatial modes. The complete time-polarization hyper-entangled states composed of two entangled

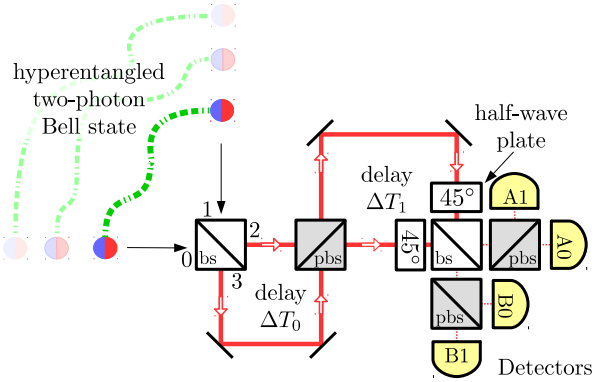

(a) Our complete Bell state measurement is achieved using linear optics and time-polarization hyperentanglement. Two-photon interference is orchestrated to ensure Bell state detection signatures do not involve two-photons coincident on a single detector. bs≡beamsplitter, pbs≡polarizing beamsplitter

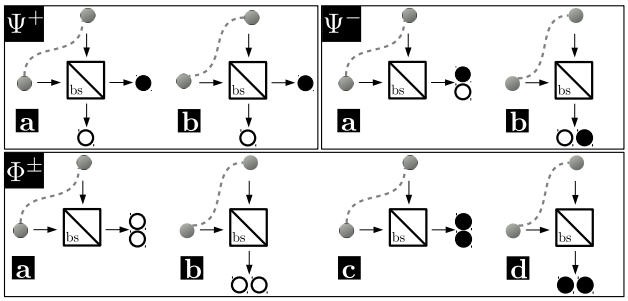

(b) Hong-Ou-Mandel interference at a beam splitter leads to unique outputs for the four Bell states. This leads to partial Bell state discrimination, perfectly identifying Ψ^+ and Ψ^- from Φ states. The Φ^+ and Φ^- states are left indistinguishable.

Figure 1

polarization qubits and one time qudit of infinite dimension are

$$\left|\Phi^{\pm}(t)\right\rangle = \left|\Phi^{\pm}\right\rangle \otimes |\,\phi(t)\rangle \tag{3}$$

$$\left|\Psi^{\pm}(t)\right\rangle = \left|\Psi^{\pm}\right\rangle \otimes |\,\phi(t)\rangle \tag{4}$$

where t is the time since photon pair creation and $\int_{-\infty}^{\infty} \langle\phi(t)|\phi(t)\rangle\, dt = 1$. The entangled photons from one of the states given in Eq. (3) or (4) enter the interferometer in Fig. 1a and output to modes 2 and 3. As shown in Fig. 1b, Hong-Ou-Mandel interference at this first beam splitter leads to a unique output for each of the four Bell state inputs. Schuck et al. suggested a similar arrangement followed by photon number resolving detection to identify the output state.

We avoid the need for photon number resolving detectors by orchestrating the two-photon interference such that our unique BSM signatures do not involve the photon pair coincident at a detector–that would require a number resolving detector to observe deterministically. Complete utilization of this interference requires the temporal modes $|\phi(t)\rangle$, $|\phi(t-\Delta T_0)\rangle$, $|\phi(t-\Delta T_1)\rangle$, and $|\phi(t-\Delta T_0-\Delta T_1)\rangle$ to be indistinguishable, which is the case when the two-photon coherence time is much larger than the apparatus paths. When this interference is present, the four Bell states have three distinct photon pair relative detection times, delays. These delays are the result of Bob's apparatus, not temporal modulations by Alice. As shown by Figs. 1a and 1b, $\Phi^{\pm}$ states result in photon pair detections with no delay between photon time of arrival. This is necessary since the photons in $\Phi^{\pm}$ states copropagate through the interferometer. By comparison, the Ψ^+ state results in a relative time delay of ΔT_0 between members of the photon pair. This is due to the members taking separate paths in the first interferometer segment and their copropagation in the second segment. A similarly unique signature for the Ψ^- state arises when those photons copropagate in the first segment and take separate paths in the second segment of the apparatus. This requires the Ψ^- photon pair to have a relative time delay of ΔT_1.

The distinct propagation for each Bell state illustrates that our apparatus is a "4-in-1" two-photon interferometer that utilizes elements from several fundamental quantum information ideas including Hong-Ou-Mandel interference,[28] partial Bell state analysis,[29] and time-entanglement.[30] Unlike previous experiments that discard a portion of the quantum coherence by segregating outputs after the first beamsplitter,[26] we retain all coherence present to assist in the complete Bell state discrimination. In conjunction with the aforementioned time signatures, the path delayed two-photon interferometers ensure unique fully determinable detection outcomes that do not include two photons with the same polarization in the same output port, a limitation of a previous experiment.[26]

We verify the design of the unique detection capabilities for this device by considering the symmetric beamsplitter relations,[26,31]

$$|H_0\rangle \overset{BS}{\rightarrow} (|H_2\rangle + i\,|H_3\rangle)/\sqrt{2} \quad |H_1\rangle \overset{BS}{\rightarrow} (i\,|H_2\rangle + |H_3\rangle)/\sqrt{2}$$
$$|V_0\rangle \overset{BS}{\rightarrow} (|V_2\,\rangle - i\,|V_3\,\rangle)/\sqrt{2} \quad |V_1\,\rangle \overset{BS}{\rightarrow} (-i\,|V_2\rangle + |V_3\rangle)/\sqrt{2}$$

where the ports $0, 1, 2$, and 3 are identified at the first beamsplitter in Fig. 1a. Additionally, the effect of a 45° polarization rotation on a single-photon using a half-wave plate, a Hadamard gate, is modeled as

$$|H\rangle \overset{45^\circ}{\rightarrow} (|H\rangle + |V\rangle)/\sqrt{2} \qquad |V\rangle \overset{45^\circ}{\rightarrow} (|H\rangle - |V\rangle)/\sqrt{2}.$$

Given these relations, one may verify that with phases $\omega\Delta T_0 = 2n\pi$ and $\omega\Delta T_1 = 2m\pi$, n and m are integers, the output states for the four Bell states given by Eqs. (3) and (4) yield the interferometer output states

$$\begin{aligned}
&\left|\Phi^+\right\rangle \rightarrow (|H_A V_A\rangle + |H_B V_B\rangle)/\sqrt{2}\\
&\left|\Phi^-\right\rangle \rightarrow (|H_A H_B\rangle - |V_A V_B\rangle)/\sqrt{2}\\
&\left|\Psi^+\right\rangle \rightarrow (|H_A H'_B\rangle + |H'_A H_B\rangle + |V_A V'_B\rangle + |V'_A V_B\rangle + |H_A V'_B\rangle - |H'_A V_B\rangle + |V_A H'_B\rangle - |V'_A H_B\rangle)/\sqrt{8}\\
&\left|\Psi^-\right\rangle \rightarrow (|H_A V''_A\rangle + |H''_A V_A\rangle - |H_B V''_B\rangle - |H''_B V_B\rangle + i\,[\,|H_A V''_B\rangle - |H''_A V_B\rangle + |V_A H''_B\rangle - |V''_A H_B\rangle])/\sqrt{8}
\end{aligned}$$

where A and B label the output ports and prime and double prime indicate a ΔT_0 and ΔT_1 delayed photon, respectively. This set of outputs is smaller than what would be observed for photons separable in the temporal degree of freedom, i.e., photons that are not hyperentangled. A time-entangled photon pair can take one of multiple paths, 2 to 4 depending on the state, but these paths are indeterminable–they interfere upon leaving the interferometer. This interference and subsequent interferometer phase sensitivity allow us to choose the deterministic and measurable Bell state detection signatures given in Table 2a. In addition to superdense coding, this novel BSM may serve as an entanglement witness for fiber-based quantum seal applications.[32]

Our experimental implementation utilized an 810 nm entangled photon pair source characterized to produce each Bell state with 0.97 fidelity. The pair source is based on spontaneous parametric down-conversion using a potassium titanyl phosphate (PPKTP) nonlinear crystal within a Sagnac loop to produce a polarization-entangled biphoton state.[33] The temporal entanglement results from the long coherence time of the continuous-wave 405 nm diode laser pump. Pumping with 1.85 mW produced 2.27×10^5 pairs/second. Alice encodes each of the four Bell states utilizing two liquid crystal waveplates. The first is oriented to apply an $I=\left(\begin{smallmatrix}1 & 0\\ 0 & 1\end{smallmatrix}\right)$ or $X=\left(\begin{smallmatrix}0 & 1\\ 1 & 0\end{smallmatrix}\right)$ gate and the second applies an I or $Z=\left(\begin{smallmatrix}1 & 0\\ 0 & -1\end{smallmatrix}\right)$ gate. Each combination II, IZ, XI, XZ encodes one of the four Bell states. Due to losses, the coincident count rate observed by Bob was approximately 200 cps.

Given our timing resolution of 4 ns we required the interferometer to have temporal delays $\Delta T_0 \approx 5$ ns and $\Delta T_1 \approx 10$ ns. Due to these large time delays, we chose to implement the experimental apparatus in polarization maintaining (PM) optical fiber as seen in Fig. 2b. The fiber lengths needed for the first loop were 1 and 2 meters, for the short and long paths, respectively, and, similarly, 2 and 4 meters in the second loop. Each fiber path consists of 2 fibers of equal length orthogonally connected such that the macroscopic temporal effects of birefringence were compensated. Experimentally, we reconfigured a simple fiber connector such that the axes were aligned orthogonally. These connections are indicated in Fig. 2b as a × symbol between two optical fibers. The use of PM optical fiber requires that we take into account the microscopic difference in phase due to birefringence in different paths. This phase compensation and the calibration of the phases needed to ensure unique BSM signatures is accomplished using liquid crystal waveplates. The phase of each photon polarization is individually modulated in the long path of the second loop and the phase of one photon polarization is modulated in the short path of the second loop. Due to the long path lengths, thermal drift of the fibers and frequency drift of the pump laser limits stable operation to approximately 100 seconds before recalibration is necessary.

We characterized the BSM performance by calibrating the interferometer to optimal discrimination settings, preparing each of the four Bell states, and recording the state detected by the apparatus. In estimating the success probabilities, we recorded approximately 800 detection signatures for each state, which occurred over a 5

Φ^+	$\Delta t = 0$, $\parallel$ ports, $\perp$ polarization
Φ^-	$\Delta t = 0$, $\perp$ ports, $\parallel$ polarization
Ψ^+	$\Delta t = \Delta T_0$, $\perp$ ports
Ψ^-	$\Delta t = \Delta T_1$, $\perp$ polarization

(a) Bell state detection signatures include a time Δt between photon detections, same or different port detection, and same ($\parallel$) or different ($\perp$) polarizations.

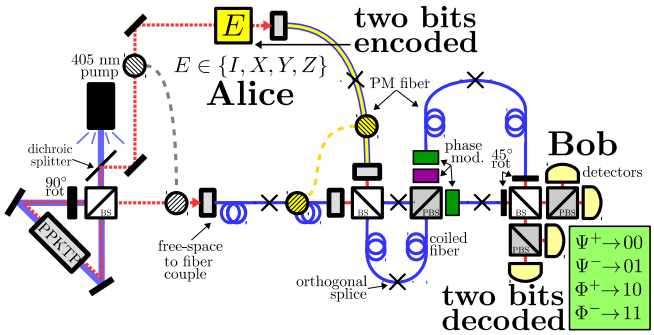

(b) To implement superdense coding, Alice and Bob initially each receive one photon from a time-polarization hyperentangled photon pair. Alice performs one of four operations on her photon which encodes two bits on the nonlocal two-photon Bell state. Alice transmits her photon to Bob who performs a Bell state measurement, i.e. decodes two bits. bs≡beamsplitter, pbs≡polarizing beamsplitter, PPKTP≡potassium titanyl phosphate.

Figure 2

Table 1: 5 s counts of received state y given sent state x.

x \ y	Φ^-	Φ^+	Ψ^-	Φ^+
Φ^-	710	8	8	4
Φ^+	7	715	9	13

x \ y	Φ^-	Φ^+	Ψ^-	Φ^+
Ψ^-	15	8	748	9
Ψ^+	34	23	15	840

second interval. The raw data collected is given in Table 1. The maximum-likelihood estimate for the conditional probabilities with accidental coincidences included are given in Fig. 2a.

The channel capacity C[34] is the maximum mutual information $I(x;y)$ possible for a given set of conditional probabilities $p(y|x)$ where x is the state prepared by Alice and y is the state decoded by Bob. This capacity is

$$C = \max_{p(\mathbf{x})} \sum_{y=0}^{3} \sum_{x=0}^{3} p(y|x)p(x) \log \left(\frac{p(y|x)}{\sum_{x'=0}^{3} p(y|x')p(x')} \right)$$

where $p(\mathbf{x}) = \{p(\Phi^-), p(\Phi^+), p(\Psi^-), p(\Psi^+)\}$ maximizes the capacity. For the conditional probabilities given in Fig. 1a we find the channel capacity to be 1.665±0.018 for arguments $p(\Phi^-)$=0.262, $p(\Phi^+)$=0.256, $p(\Psi^-)$=0.256, and $p(\Phi^+)$=0.226. The maximum channel capacity possible using linear optics, a single-qubit, and a single degree of entanglement is 1.585 *. Our experiment has exceeded this bound as well as the previous highest channel capacity reported for encoding on a single-qubit and decoding using linear optics.[24]

We next demonstrate the use of superdense coding as part of a hybrid, quantum-classical protocol for communicating between users Alice and Bob. We make use of conventional optical network communication between two users to coordinate Alice's quantum transmitter and Bob's quantum receiver.[36,37] The basic steps in the protocol for this demonstration are:

1. Alice transmits a classical send request to Bob.
2. Bob returns a classical acknowledgement to Alice.
3. Alice transmits two bits using superdense coding.
4. Bob receives and decodes the two-bit message.
5. Bob transmits a classical receipt to Alice.

*We note that methods have been proposed to achieve a channel capacity of 2 utilizing linear optics and one photon on average.[35]

This protocol is repeated n times until Alice has completed transmission of a $2n$-bit message to Bob. Due to the spontaneous nature of the photon pair source, only the first photon-pair detected during step 3 above is used even though other photon pairs may be detected. In this regard, the classical messages before and after a burst of superdense coding act to frame each two-bit message. While this incurs a large overhead, it ensures the detected bits are properly framed so that the transmitted message can be reliably constructed. A less conservative protocol would permit Alice to transmit multiple two-bit messages uninterrupted and require Bob to properly partition this sequence into the corresponding frames.

3. IMAGE TRANSFER APPLICATION

As a demonstration of the system capabilities, we have transmitted the 3.4 kB image shown in Fig. 3b(left). The corresponding received image is shown in Fig. 3b(right). The received image is calculated to have a fidelity of 87%. The errors in the received image result from drift in the interferometer during transmission, phase miscalibration, and imperfect state generation. It should be apparent that the fidelity of the received image is less than that of the optimal characterization presented in Fig. 3a. This is due to performance trade-offs in system operation that reduce the collection time at the expense of reduced detection fidelity. For the current demonstration the effective bit rate during operation that included a classical send message, phase encoding using liquid crystal waveplates, a classical receive message, and periodic calibration was 1 bit/sec. The fiber link for this system was 2 meters of PM optical fiber. We do not foresee any fundamental impediments to using longer optical fibers beyond increased losses and cost. In particular, an implementation using standard single-mode fiber could operate by using a polarization correction or stabilization system.

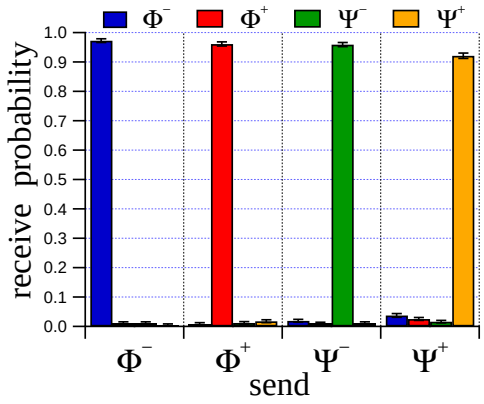

(a) The conditional probabilities $p(y|x)$ of receiving state y given the sent state x using our apparatus gives the highest channel capacity to date, 1.665±0.018, by encoding on a single-qubit and decoding using linear optics.

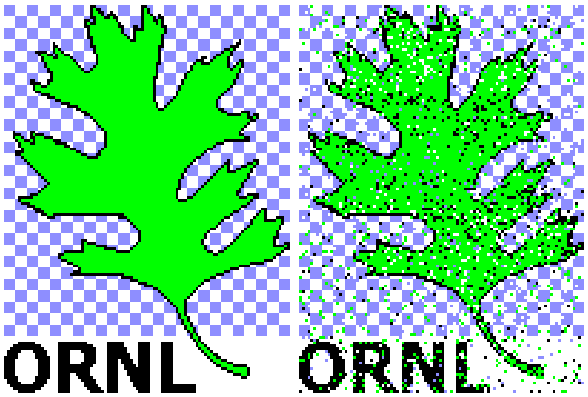

(b) (Left): The original 4-color 100x136 pixel 3.4kB image. (Right): The image received using superdense coding. The calculated fidelity was 87%.

Figure 3

Our experiment could be improved by reducing the spontaneity of the source by utilizing a pulsed pump laser, in which case the temporal delays in the interferometer would need to be multiples of the pulse period t_p, for instance $\Delta T_0 = t_p$ and $\Delta T_1 = 2t_p$. Achieving a finer time resolution would allow for smaller delays ΔT_0 and ΔT_1 which would improve the stability, i.e. the drift would be reduced. Packaging the device or using integrated optics would substantially increase the bit-rate by reducing the photon pair loss due to free-space to fiber coupling inefficiencies. The speed of Alice's encoding is limited by the response time of the liquid crystal waveplates which is on the order of milliseconds. Faster options include lithium-niobate phase modulators[38] which can achieve modulation speeds on the order of nanoseconds.

4. CONCLUSION

In conclusion, we have achieved a single-qubit channel capacity of 1.665 ± 0.018 over optical fiber links enabled by a complete BSM using linear optics, hyperentanglement, and common single-photon detectors. This channel capacity is the highest to date for encoding on a single-qubit and decoding using linear optics. Our novel interferometric design allows "off-the-shelf" single-photon detectors to enable the complete Bell state discrimination instead of the number-resolving detectors required by previous experiments.[26] To our knowledge, this is the first demonstration of superdense coding over optical fiber and a step towards practical realization of superdense coding. We further used this implementation to demonstrate an image transfer application between end users as an example of a quantum networking environment. Future improvements can take advantage of error correction methods, including conventional forward error correction,[37] to improve the transmission fidelity. These demonstration of a hybrid quantum-classical transfer protocol represents a step toward the future integration of quantum communication with fiber-based networks.[39,40]

REFERENCES

[1] Nielsen, M. A. and Chuang, I. L., [*Quantum Computation and Quantum Information: 10th Anniversary Edition*], Cambridge University Press (2011).

[2] Kimble, H. J., "The quantum internet," *Nature* **453**(7198), 1023–1030 (2008).

[3] Van Meter, R., [*Quantum Networking*], John Wiley and Sons (2014).

[4] Dasari, V. R., Sadlier, R. J., Prout, R., Williams, B. P., and Humble, T. S., "Programmable multi-node quantum network design and simulation," *Proc. SPIE* **9873**, 98730B (2016).

[5] Elliott, C., "Building the quantum network," *New Journal of Physics* **4**(1), 46 (2002).

[6] Lnger, T. and Lenhart, G., "Standardization of quantum key distribution and the etsi standardization initiative isg-qkd," *New Journal of Physics* **11**(5), 055051 (2009).

[7] Scheidl, T., Ursin, R., Fedrizzi, A., Ramelow, S., Ma, X.-S., Herbst, T., Prevedel, R., Ratschbacher, L., Kofler, J., Jennewein, T., and Zeilinger, A., "Feasibility of 300km quantum key distribution with entangled states," *New Journal of Physics* **11**(8), 085002 (2009).

[8] Chapuran, T. E., Toliver, P., Peters, N. A., Jackel, J., Goodman, M. S., Runser, R. J., McNown, S. R., Dallmann, N., Hughes, R. J., McCabe, K. P., Nordholt, J. E., Peterson, C. G., Tyagi, K. T., Mercer, L., and Dardy, H., "Optical networking for quantum key distribution and quantum communications," *New Journal of Physics* **11**(10), 105001 (2009).

[9] Chen, T.-Y., Wang, J., Liang, H., Liu, W.-Y., Liu, Y., Jiang, X., Wang, Y., Wan, X., Cai, W.-Q., Ju, L., Chen, L.-K., Wang, L.-J., Gao, Y., Chen, K., Peng, C.-Z., Chen, Z.-B., and Pan, J.-W., "Metropolitan all-pass and inter-city quantum communication network," *Opt. Express* **18**, 27217–27225 (Dec 2010).

[10] Weigel, W. and Lenhart, G., "Standardization of quantum key distribution in etsi," *Wirel. Pers. Commun.* **58**(1), 145–157 (2011).

[11] Elkouss, D., Martinez-Mateo, J., Ciurana, A., and Martin, V., "Secure optical networks based on quantum key distribution and weakly trusted repeaters," *J. Opt. Commun. Netw.* **5**, 316–328 (Apr 2013).

[12] Wu, D., Yu, W., Zhao, B., and Wu, C., "Quantum key distribution in large scale quantum network assisted by classical routing information," *International Journal of Theoretical Physics* **53**(10), 3503–3511 (2014).

[13] Ciurana, A., Martin, V., Martinez-Mateo, J., Schrenk, B., Peev, M., and Poppe, A., "Entanglement distribution in optical networks," *IEEE Journal of Selected Topics in Quantum Electronics* **21**, 37–48 (May 2015).

[14] Humble, T. S. and Sadlier, R. J., "Software-defined quantum communication systems," *Optical Engineering* **53**(8), 086103 (2014).

[15] Williams, B. P., Sadlier, R. J., and Humble, T. S., "Superdense coding over optical fiber links with complete bell-state measurements," *Phys. Rev. Lett* **118**, 050501 (2017).

[16] Bennett, C. H. and Wiesner, S. J., "Communication via one- and two-particle operators on einstein-podolsky-rosen states," *Phys. Rev. Lett.* **69**, 2881–2884 (Nov 1992).

[17] Lvovsky, A. I., Sanders, B. C., and Tittel, W., "Optical quantum memory," *Nature photonics* **3**(12), 706–714 (2009).

[18] Lütkenhaus, N., Calsamiglia, J., and Suominen, K.-A., "Bell measurements for teleportation," *Physical Review A* **59**(5), 3295 (1999).
[19] Vaidman, L. and Yoran, N., "Methods for reliable teleportation," *Phys. Rev. A* **59**, 116–125 (Jan 1999).
[20] Kim, Y.-H., Kulik, S. P., and Shih, Y., "Quantum teleportation of a polarization state with a complete bell state measurement," *Physical Review Letters* **86**(7), 1370 (2001).
[21] Grice, W. P., "Arbitrarily complete bell-state measurement using only linear optical elements," *Physical Review A* **84**(4), 042331 (2011).
[22] Kwiat, P. G., "Hyper-entangled states," *Journal of modern optics* **44**(11-12), 2173–2184 (1997).
[23] Barreiro, J. T., Langford, N. K., Peters, N. A., and Kwiat, P. G., "Generation of hyperentangled photon pairs," *Phys. Rev. Lett.* **95**, 260501 (Dec 2005).
[24] Barreiro, J. T., Wei, T.-C., and Kwiat, P. G., "Beating the channel capacity limit for linear photonic superdense coding," *Nature physics* **4**(4), 282–286 (2008).
[25] Barbieri, M., Vallone, G., Mataloni, P., and De Martini, F., "Complete and deterministic discrimination of polarization bell states assisted by momentum entanglement," *Physical Review A* **75**(4), 042317 (2007).
[26] Schuck, C., Huber, G., Kurtsiefer, C., and Weinfurter, H., "Complete deterministic linear optics bell state analysis," *Physical review letters* **96**(19), 190501 (2006).
[27] Dasari, V. R., Sadlier, R. J., Prout, R., Williams, B. P., and Humble, T. S., "Programmable multi-node quantum network design and simulation," *Proc. SPIE* **9873**, 98730B–98730B–9 (2016).
[28] Hong, C. K., Ou, Z. Y., and Mandel, L., "Measurement of subpicosecond time intervals between two photons by interference," *Phys. Rev. Lett.* **59**, 2044–2046 (Nov 1987).
[29] Weinfurter, H., "Experimental bell-state analysis," *EPL (Europhysics Letters)* **25**(8), 559 (1994).
[30] Franson, J. D., "Bell inequality for position and time," *Physical Review Letters* **62**(19), 2205 (1989).
[31] Ou, Z.-Y. J., [*Multi-photon quantum interference*], Springer (2007).
[32] Williams, B. P., Britt, K. A., and Humble, T. S., "Tamper-indicating quantum seal*," *Phys. Rev. Applied* **5**, 014001 (Jan 2016).
[33] Kim, T., Fiorentino, M., and Wong, F. N. C., "Phase-stable source of polarization-entangled photons using a polarization sagnac interferometer," *Phys. Rev. A* **73**, 012316 (Jan 2006).
[34] Cover, T. M. and Thomas, J. A., [*Elements of information theory*], John Wiley & Sons (2012).
[35] Lougovski, P. and Uskov, D. B., "Channel-capacity gain in entanglement-assisted communication protocols based exclusively on linear optics, single-photon inputs, and coincidence photon counting," *Phys. Rev. A* **92**, 022303 (Aug 2015).
[36] Humble, T. S. and Sadlier, R. J., "Software-defined quantum communication systems," *Optical Engineering* **53**(8), 086103 (2014).
[37] Sadlier, R. J. and Humble, T. S., "Superdense coding interleaved with forward error correction," *Quantum Measurements and Quantum Metrology* **3**, 1 (2016).
[38] Wooten, E. L., Kissa, K. M., Yi-Yan, A., Murphy, E. J., Lafaw, D. A., Hallemeier, P. F., Maack, D., Attanasio, D. V., Fritz, D. J., McBrien, G. J., and Bossi, D. E., "A review of lithium niobate modulators for fiber-optic communications systems," *IEEE Journal of Selected Topics in Quantum Electronics* **6**, 69–82 (Jan 2000).
[39] Humble, T. S., "Quantum security for the physical layer," *Communications Magazine, IEEE* **51**(8), 56–62 (2013).
[40] Dasari, V. R. and Humble, T. S., "Openflow arbitrated programmable network channels for managing quantum metadata," *J. Defense Modeling and Simulation* **13**, arXiv:1512.08545 (2015).